JOURNAL OF SPECTROSCOPY AND DYNAMICS

Ultrafast 2D NMR applied to the kinetic study of D-glucose mutarotation in aqueous solution

Patrick Giraudeau*, Pauline Lemeunier, Mathieu Coutand, Jean-Marie Doux, Alexis Gilbert, Gérald S. Remaud, Serge Akoka

Université de Nantes, CNRS, Chimie et Interdisciplinarité: Synthèse, Analyse, Modélisation (CEISAM) UMR 6230, B.P. 92208, 2 rue de la Houssinière, F-44322 Nantes Cedex 03, France

Author for correspondence: Patrick Giraudeau, email: patrick.giraudeau@univ-nantes.fr
Received 20 Dec 2010; Accepted 25 Jan 2011; Available Online 22 Mar 2011

Abstract

Two-dimensional Nuclear Magnetic Resonance (2D NMR) is hampered by long acquisition times. Consequently, 2D NMR is ill-suited for the study of short timescale phenomena such as kinetic studies or dynamic processes. Fortunately, ultrafast 2D NMR makes it possible to record a 2D NMR correlation in a single scan, and is therefore adapted to real-time studies of fast occurring processes. Here, we describe the application of heteronuclear ultrafast 2D NMR to the kinetic study of D-glucose mutarotation at natural abundance in non-deuterated water. Mutarotation constants are determined with a 10% precision. The results presented in this paper are a new illustration of the potentialities of ultrafast 2D NMR for real-time kinetic studies.

Keywords: 2D NMR; Ultrafast NMR; HSQC; Kinetics; Mutarotation; Glucose

1. Introduction

One-dimensional (1D) ^{1}H nuclear magnetic resonance (NMR) is a powerful tool for analytical applications in a wide variety of domains, from drug analysis [1], to natural products analysis [2], or *in vivo* spectroscopy [3]. However, the analysis of complex mixtures often fails in the case of large molecules or complex mixtures, due to the large overlap between peaks characterizing one-dimensional ^{1}H NMR spectra. Heteronuclear NMR is a valuable alternative, however it suffers from a low sensitivity due to the natural abundance and to the low gyromagnetic ratio of common heteronuclei such as ^{13}C or ^{15}N. Two-dimensional (2D) NMR [4,5], offers a solution to the limitations of 1D NMR, as it brings a resolution enhancement that is essential for quantitative studies of complex spectra. However, its main drawback is the duration of the experiments (up to several hours), necessary to acquire the whole 2D FID, due to the necessary repetition of numerous transients with incremented delays. Because of this time constraint, 2D NMR is ill-suited for studying dynamic phenomena occurring on a short timescale, such as chemical exchange, protein folding or more generally kinetics of fast chemical reactions. Conventional 2D NMR experiments are also incompatible with techniques presenting an irreversible character such as dissolution Dynamic Nuclear Polarization [6].

In the last ten years, NMR spectroscopists have proposed a number of strategies [7-11], to overcome this time limitation and to obtain 2D NMR spectra in a much reduced time. The most efficient of these strategies is probably the ultrafast 2D NMR approach recently proposed by L. Frydman and co-workers [12,13], where the acquisition of 2D NMR spectra is carried out in a single scan. To achieve this performance, the usual indirect-domain temporal encoding of conventional 2D NMR is replaced by a spatial encoding scheme followed by a conventional mixing period and by a detection block based on Echo Planar Imaging (EPI) [14]. When an appropriate mixing period is employed, any type of homo- or heteronuclear correlation can be observed after an adapted post-processing [12]. The principles of ultrafast techniques, as well as their experimental implementation, have been described in detail in recent literature [15-17].

Ultrafast 2D NMR initially suffered from important limitations in terms of resolution, sensitivity and spectral width [18-21], but over the last few years, several significant methodological improvements have increased its performances significantly [18, 21-25], making it suitable for analyzing mixtures with increasing complexity. In particular, the gradient-controlled folding procedure that we recently proposed [25], makes it possible to access large spectral

widths at no cost, thus allowing the acquisition of heteronuclear ultrafast 2D spectra with large ^{13}C ranges. Moreover, we showed recently that ultrafast 2D NMR under such optimized conditions formed a valuable tool for precise quantitative analysis [26].

Recent papers have highlighted the potentialities of ultrafast 2D NMR to follow kinetics of chemical reactions occuring on a short timescale [27-29]. Homonuclear ultrafast pulse sequences such as Total Correlation Spectroscopy (TOCSY) have been successfully applied to real-time monitoring of organic reactions [29], and very recently, Herrera *et al.* reported the first application of ultrafast heteronuclear 2D NMR to follow structural changes on a carbonyl carbon atom [28]. However, this application was limited to ^{13}C-labeled compounds as highlighted by the authors. Moreover, all the kinetic studies followed by ultrafast 2D NMR have been limited to reactions in deuterated solvents [27-29].

In this paper, we describe the application of heteronuclear ultrafast 2D NMR to the study of D-glucose mutarotation in water. The ability of ultrafast 2D NMR to study dynamic processes is demonstrated in non-deuterated water at natural ^{13}C abundance.

2. Experimental

2.1. Sample preparation

For the initial setting of ultrafast experiments and for the acquisition of the conventional HSQC spectrum (Figure 3), a D-glucose solution was obtained by dissolving 270 mg of D-glucose in 750 µL of D_2O. The sample was filtered and transferred in a 5 mm tube after several hours for analysis, to make sure that the mutarotation equilibrium was reached.

For the kinetic studies, 270 mg of D-glucose were rapidly dissolved at $t = 0$ in 750 µL of H_2O at room temperature (298 K). After complete dissolution, the sample was filtered and transferred into a 5 mm tube.

2.2. NMR acquisition

NMR spectra were recorded at 298 K on a Bruker Avance I 400 spectrometer, at a ^1H frequency of 400.13 MHz with a 5 mm dual+ probe equipped with *z*-axis gradients. Conventional 1D and 2D experiments were recorded with routine pulse sequences available within the commercial software Bruker Topspin 2.1. The conventional HSQC spectrum was recorded with 256 t_1 increments, 4 scans, a recovery delay of 5 s and an acquisition time of 1 s. ^1H longitudinal relaxation times were determined by a standard inversion-recovery pulse sequence with variable delays ranging from 0.1 s to 5 s.

For ultrafast HSQC experiments, the spatial encoding was performed using a constant-time spatial encoding scheme [23], with 15 ms smoothed chirp [30], encoding pulses. The sweep range for the encoding pulses (57 kHz for HSQC) was set to be significantly larger than the chemical shift range, and the amplitude of the encoding gradients was adapted to obtain a frequency dispersion equivalent to the frequency range of the pulses (G_e = 26.9 G/cm). The INEPT delays in the pulse sequence were set to 1.56 ms, corresponding to $1/(4<J_{CH}>)$. Additional "folding" gradients were set to optimize peak folding along the ultrafast dimension, with the following amplitude and duration values: G_1:-12.5 G.cm^{-1}; 0.5 ms, G_2: 3.8 G.cm^{-1}; 1 ms. Acquisition gradient parameters were set as follows: G_a = 52.8 G/cm, T_a = 258.5 µs, 128 detection gradient pairs.

For the kinetic studies, after fast dissolution as described above, the sample was transferred to the spectrometer within 4 minutes after beginning the dissolution. Then, 2 additional minutes were allowed for stabilization of the sample and fast shimming. The first acquisition was performed 6 minutes after dissolution. Then, ultrafast spectra were recorded every 3 minutes with 16 scans and a 2 step phase cycling (180° phase alternation on the last ^{13}C 90° pulse and on the receiver). Spectra were recorded during *c.a.* 200 min after dissolution. The spectrometer lock was inactive during the whole experiment, as the sample was devoid of deuterated solvent. As a consequence, the peaks were slightly shifted in the course of the whole experiment; this shift was taken into account when integrating 2D peaks.

2.3. NMR processing

All the spectra were analysed using the Bruker program Topspin 2.1. Inversion-recovery experiments were analysed within the Bruker software for the dermination of T_1 values. The specific processing for ultrafast spectra (as described in Ref. [12]) was performed using our home-written routine in Topspin. The processing included an exponential apodization (LB = 3 Hz) in the conventional dimension and zero-filling to 1k. An automatic polynomial (n = 3) baseline correction was applied in the conventional dimension in the region containing the peaks used for quantification.

2D peak volumes were integrated by using MestRe-C 4.7 with integration regions adjusted to the relevant peaks. Relative concentrations were obtained by calculating relative peak volumes from anomeric cross-peaks, and plotted as a function of time. All data

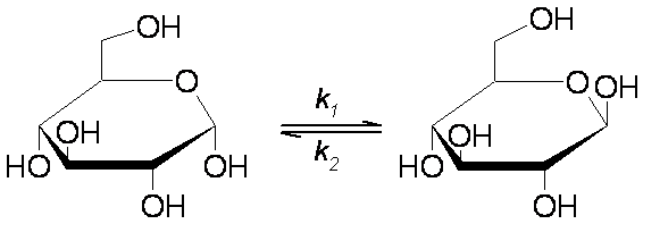

Figure 1. D-glucose mutarotation equilibrium, characterized by forward (k_1) and reverse (k_2) mutarotation rate constants.

analysis were carried out in Microsoft Excel. Fitting to a theoretical model by a least-square procedure using Microsoft Excel Solver allowed the determination of kinetic rate constants.

3. Results and Discussion

3.1. Observation of the D-glucose mutarotation

When α-D-glucose is dissolved in solution, it undergoes a mutarotation reaction as described in Figure 1, until the equilibrium between α- and β- anomers is reached. The mutarotation equilibrium was discovered in 1846 [31], however the kinetics of monosaccharide mutarotation is still the purpose of current research, as described in many recent papers [32-36]. The main methodologies used to follow the kinetics of mutarotation are divided into 3 categories: chromatography (requiring prior derivatization) [32], optical polarimetric methods [36] and NMR [35]. The latter is probably the more generally applicable of these methods, however NMR studies of mutarotation reactions have been limited to deuterated solvents [35], as strong proton signals originating from the solvent peaks strongly affect the precision of the method. It is particularly true when saccharides are dissolved in water, as described in Figure 2, which shows the ^{1}H NMR spectrum of D-glucose in H_2O. ^{1}H NMR peaks between 3.0 and 3.7 ppm are not significanlty affected by the water peak, however the signal overlap in this region is too large to allow precise quantitative measurements. Signals arising from anomeric protons are clearly separated, but peak areas are strongly affected by the solvent signal, as clearly visible in Figure 2. Due to their proximity to the water signal, these peaks would be affected by water presaturation. For these reasons, the study of glucose by NMR in non-deuterated solvents has never been reported to our knowledge.

This limitation could be bypassed by employing quantitative ^{13}C NMR [37], as the large ^{13}C chemical shift range considerably reduces the signal overlap. However, ^{13}C NMR suffers from long experiment times due to the inherent low sensitivity of ^{13}C-detected experiments and to the long ^{13}C longitudinal relaxation times (T_1).

A promising alternative to benefit from the large chemical shift dispersion of ^{13}C NMR while preserving a good sensitivity is the use of ^{1}H-detected heteronuclear 2D NMR spectroscopy, whose most widespread implementation is the Heteronuclear Single Quantum Correlation (HSQC) experiment [38]. Figure 3 shows the conventional ^{1}H-^{13}C HSQC spectrum of a D-glucose solution in D_2O, where clearly separated signals originating from the two anomers could potentially be used for quantification. Unfortunately, it is evident that

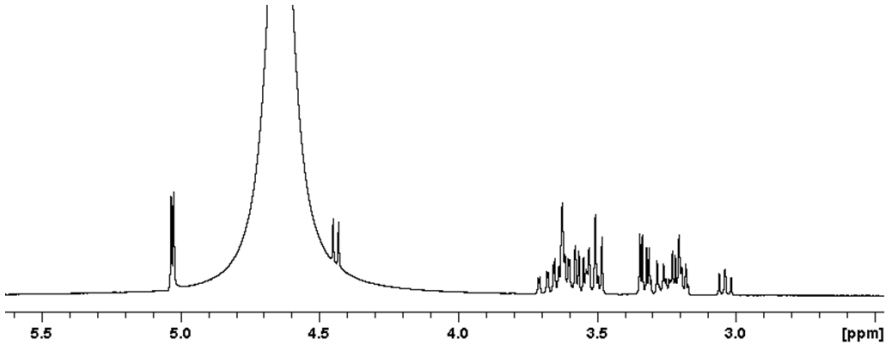

Figure 2. ^{1}H NMR spectrum of D-glucose in H_2O, recorded at 298 K and 400.13 MHz. The spectrum was recorded several hours after preparing the sample, thus ensuring that the mutarotation equilibrium was reached. The water signal was truncated vertically.

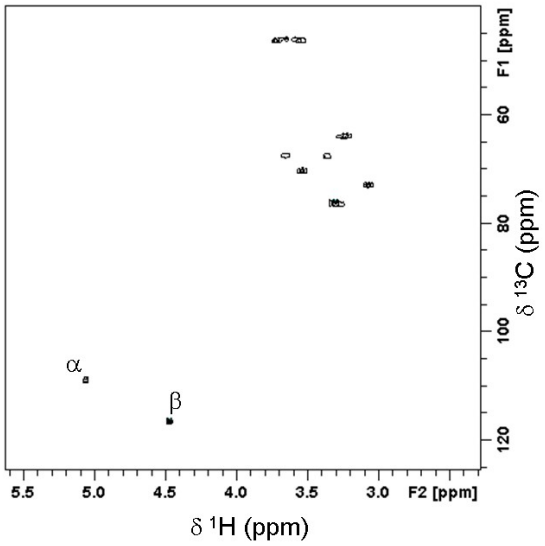

Figure 3. 2D HSQC NMR spectrum of D-glucose in H_2O, recorded at 298 K and 400.13 MHz. The spectrum was recorded in 1 h 45 min, several hours after preparing the sample, thus ensuring that the mutarotation equilibrium was reached. Signals arising from anomeric ^{1}H-^{13}C pairs are indicated close to the corresponding peaks.

the long experiment duration required to record a 2D correlation is not compatible with the timescale of glucose mutarotation, as the equilibrium is reached in approximately 3 h [32]. Even under optimized conditions, it was shown recently that the duration of a quantitative 2D HSQC experiment could not be decreased under 12 min [39], which is still not really adapted to the timescale involved here.

3.2. Heteronuclear ultrafast 2D NMR

With these considerations as background, we set out to explore the potentialities of ultrafast 2D NMR for studying D-glucose mutarotation in real time. We implemented an ultrafast HSQC pulse sequence (Figure 4A) that we recently described [25], including a constant-time phase-encoding pattern initially proposed by Pelupessy [23], as well as additional gradients on each side of the mixing period to allow folding in the ultrafast dimension, following the procedure described in Ref. [25]. In order to obtain optimum conditions for quantitative analysis [26], acquisition parameters were optimized to reach the best compromise between sensitivity and resolution. To obtain a better sensitivity, 16 scans were recorded with a recovery delay of 5 s, corresponding to $5 \cdot T_1^{max}$, where T_1^{max} is the highest ^{1}H longitudinal relaxation time. These conditions ensure that intensity distortions due to ^{1}H relaxation are lower than 0.7% [40].

The ultrafast spectrum of D-glucose in H_2O at equilibrium, recorded in 1 min 22 s, is shown in Figure 4B. All the expected peaks are present compared to the conventional spectrum in Figure 3. A noticeable aspect of the ultrafast spectrum is that the signals from anomeric protons are folded along the spatial-encoding (vertical) dimension in order to decrease the demand on gradient amplitudes [25]. This folding is not a limiting obstacle, as folded peaks do not overlap with other signals. Another important observation is the absence of signal arising from the solvent, even though the spectrum has been acquired in non-deuterated water. This is due to the coherence-selection ensured by i) a two-step phase cycling consisting of a 180° phase alternation on the last ^{13}C 90° pulse and on the receiver; ii) the gradient scheme implemented in the pulse sequence. Thanks to these features, signals from ^{1}H not bound to ^{13}C are totally eliminated from the HSQC spectrum.

The experiment duration could of course be decreased by working at higher fields and/or with a cryogenic probe, options that were not available in our lab at the time of the study. However, the acquisition time is perfectly compatible with short timescale kinetic studies, as an HSQC spectrum can now be recorded every 1.5 minutes.

3.3. Kinetic study

The kinetic study of D-glucose mutarotation in water was performed by recording a series of ultrafast HSQC spectra in the conditions described above. Thanks to a fast dissolution and to preliminary spectrometer settings as described in the experimental part, we were able to start the acquisition no later than 6

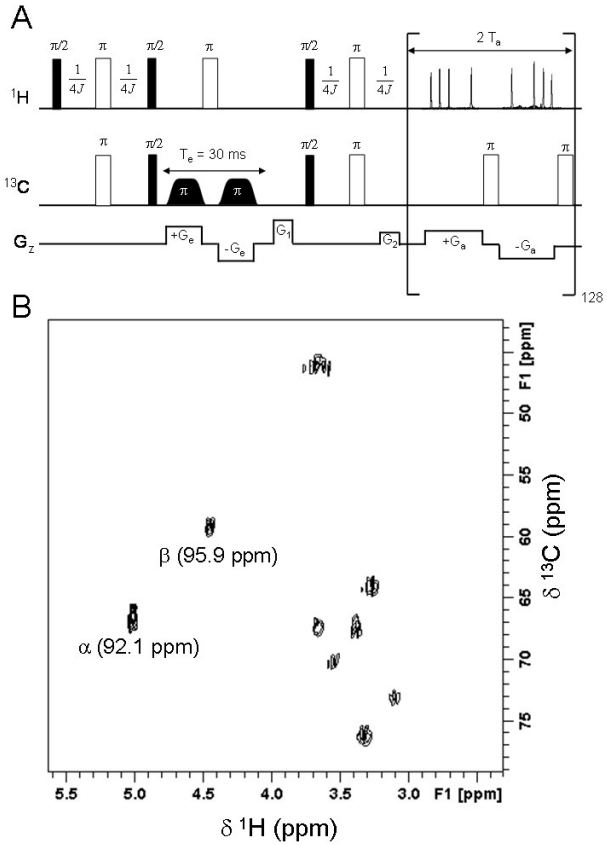

Figure 4. Ultrafast 2D HSQC pulse sequence (A) and corresponding spectrum (B), recorded at 298 K and 400.13 MHz, after reaching mutarotation equilibrium. 16 transients were recorded, resulting in a total acquisition time of 1 min 22 s. Relevant acquisition parameters are indicated in the experimental part. Signals arising from anomeric ^{1}H-^{13}C pairs, indicated close to the corresponding peaks, were folded in the ultrafast dimension by adjusting G_1 and G_2 gradients. Their actual chemical shift is indicated.

minutes after beginning the dissolution of D-glucose in water. Here, we chose to record an HSQC spectrum every 3 min, a value that appeared more than sufficient to properly characterize the mutarotation kinetics. For all spectra, the relative concentrations of α- and β-anomers were determined by calculating the relative peak volumes of anomeric cross peaks indicated on Figure 4.

The evolution of concentrations in the course of time is plotted in Figure 5, showing that the equilibrium is reached in *c.a.* 3 hours, as reported in a previous study carried out in similar conditions [32].

Assuming a first-order kinetic law, the rate equation of mutarotation is given by:

$$-\frac{dc^{\alpha}(t)}{dt}=\frac{dc^{\beta}(t)}{dt}=k_1c^{\alpha}(t)-k_2c^{\beta}(t) \quad (1)$$

as described in Ref. [36], where $c^{\alpha}(t)$ and $c^{\beta}(t)$ are the time-dependant concentrations of α- and β- anomers, respectively, and k_1 and k_2 the forward and reverse mutarotation rate constants, as described in Figure 1. Integration of Equation. (1) leads to the following expression of the relative concentration of the α anomer in the course of time:

$$\frac{c^{\alpha}(t)}{c^{\alpha}(t)+c^{\beta}(t)}=\frac{k_2}{k_1+k_2}+\frac{k_1}{k_1+k_2}e^{-(k_1+k_2)t} \quad (2)$$

A similar expression can be obtained for $c^{\beta}(t)$, as the sum of the relative concentrations is equal to 1.

The experimental values of relative concentrations (Figure 5) were fitted to this model by a least-square procedure, resulting in an excellent adequacy between the model and the experimental results. The corresponding rate constants were obtained as follows: $k_1 = 8.9 \times 10^{-5} \pm 0.9 \times 10^{-5}$ s^{-1} and $k_2 = 5.4 \times 10^{-5} \pm 0.6 \times 10^{-5}$ s^{-1}. These values are the average of 3 experiments repeated over a two-week interval, and the associated standard deviations were also calculated from the k_1 and k_2 values obtained for these 3 experiments. The coefficients of variation for k_1 and k_2 are close to 10%, which confers our method a good repeatability. From

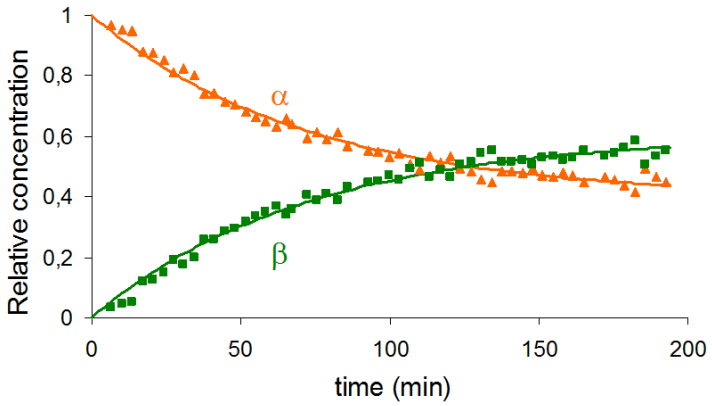

Figure 5. Mutarotation kinetics of D-glucose dissolved in water. Relative concentrations were obtained by calculating relative peak volumes from anomeric cross-peaks on ultrafast 2D HSQC spectra, and plotted as a function of time. The initial time corresponds to the instant when the dissolution of glucose in water started. Solid lines represent the adjustment to a first-order kinetic law as described in the text.

the values of k_1 and k_2, the equilibrium constant K_m can also be calculated by $K_m = k_1/k_2 = 1.6$.

The mutarotation rate constants and the equilibrium constant obtained by ultrafast 2D NMR are of the same order of magnitude as those obtained in previous studies by optic polarimetry [36], chromatography [32], or theoretical studies [33]. The precise comparaison between numeric values is not fully relevant as the different studies were not carried out under identical conditions (solvent, temperature, etc.). However, the difference between our values and the ones reported in other studies is not higher than the difference between those studies themselves.

An interesting feature of the method described in this paper is that its implementation on routine spectrometers is relatively straightforward, as it does not require specific hardware apart from a *z*-gradient probe. All the spectra presented here were acquired on a commercial 400 MHz spectrometer equipped with standard hardware.

4. Conclusions

The results presented in this paper are a new illustration of the potentialities of ultrafast 2D NMR for real-time kinetic studies. The study is carried out at ^{13}C natural abundance in a non-deuterated solvent. This result opens valuable perspectives for future kinetic studies by ultrafast 2D NMR. The application to a reaction involving saccharides opens the way to future studies involving more complex species such as mutarotation of polysaccharides or enzymatic reactions. More systematic studies considering the influence of experimental parameters, such as temperature or solvent, will be carried out to investigate the analytical potentialities (robustness, precision, repeatability) of ultrafast 2D NMR under various experimental conditions.

Acknowledgements

The authors are grateful to Michel Giraudeau for linguistic assistance.

References

1. U. Holzgrabe, J. Pharm. Biomed. Anal. 38 (2005) 806.
2. G.F. Pauli, B.U. Jaki, D.C. Lankin, J. Nat. Prod. 68 (2005) 133.
3. F. Podo, O. Henriksen, W.M.M.J. Bovée, M.O. Leacj, D. Leibfritz, J.D. De Certaines, Magn. Reson. Imaging 16 (1998) 1085.
4. W.P. Aue, E. Bartholdi, R.R. Ernst, J. Chem. Phys. 64 (1976) 2229.
5. J. Jeener, Lecture presented at Ampere International Summer School II, Basko Polje, Yugoslavia (1971).
6. J.H. Ardenkjaer-Larsen, B. Fridlund, A. Gram, G. Hansson, L. Hansson, M.H. Lerche, R. Servin, M. Thaning, K. Golman, Proc. Natl. Acad. Sci. U.S.A. 100 (2003) 10158.
7. P. Schanda, B. Brutscher, J. Am. Chem. Soc. 127 (2005) 8014.
8. E. Kupce, R. Freeman, J. Magn. Reson. 162 (2003) 300.
9. A.S. Stern, K.-B. Li, J.C. Hoch, J. Am. Chem. Soc. 124 (2002) 1982.
10. E. Kupce, R. Freeman, J. Am. Chem. Soc. 126 (2004) 6429.
11. R. Brüschweiler, F. Zhang, J. Chem. Phys. 120 (2004) 5253.
12. L. Frydman, A. Lupulescu, T. Scherf, J. Am. Chem. Soc. 125 (2003) 9204.
13. L. Frydman, T. Scherf, A. Lupulescu, Proc. Natl. Acad. Sci. USA 99 (2002) 15858.

14. P. Mansfield, Magn. Reson. Med. 1 (1984) 370.
15. M. Gal, L. Frydman, Ultrafast Multidimensional NMR: Principles and Practice of Single-scan Methods, In: D.M. Grant, R.K. Harris (Eds.), Encyclopedia of NMR, Wiley, New York (2009).
16. M. Mishkovsky, L. Frydman, Annu. Rev. Phys. Chem. 60 (2009) 429.
17. A. Tal, L. Frydman, Prog. Nucl. Magn. Reson. Spectrosc. 57 (2010) 241.
18. P. Giraudeau, S. Akoka, J. Magn. Reson. 190 (2008) 339.
19. P. Giraudeau, S. Akoka, J. Magn. Reson. 192 (2008) 151.
20. P. Giraudeau, S. Akoka, J. Magn. Reson. 195 (2008) 9.
21. Y. Shrot, L. Frydman, J. Chem. Phys. 128 (2008) 164513.
22. Y. Shrot, B. Shapira, L. Frydman, J. Magn. Reson. 171 (2004) 163.
23. P. Pelupessy, J. Am. Chem. Soc. 125 (2003) 12345.
24. P. Pelupessy, L. Duma, G. Bodenhausen, J. Magn. Reson. 194 (2008) 169.
25. P. Giraudeau, S. Akoka, J. Magn. Reson. 205 (2010) 171.
26. P. Giraudeau, G.S. Remaud, S. Akoka, Anal. Chem. 81 (2009) 479.
27. M. Gal, M. Mishkovsky, L. Frydman, J. Am. Chem. Soc. 128 (2006) 951.
28. A. Herrera, E. Fernandez-Valle, E.M. Gutiérrez, R. Martinez-Alvarez, D. Molero, Z.D. Pardo, E. Saez, Org. Lett. 12 (2010) 144.
29. A. Herrera, E. Fernández-Valle, R. Martínez-Álvarez, D. Molero, Z.D. Pardo, E. Sáez, M. Gal, Angew. Chem. Int. Edit. 48 (2009) 6274.
30. J.M. Böhlen, G. Bodenhausen, J. Magn. Reson. A 102 (1992) 293.
31. C.S. Hudson, J. Am. Chem. Soc. 32 (1910) 889.
32. N. Le Barc'H, J.M. Grossel, P. Looten, M. Mathlouthi, Food Chem. 74 (2001) 119.
33. A.M. Silva, E.C. da Silva, C.O. da Silva, Carbohydr. Res. 341 (2006) 1029.
34. J.A. Beebe, A. Arabshahi, J.G. Clifton, D. Ringe, G. Petsko, P.A. Frey, Biochemistry 42 (2003) 4414.
35. K.-S. Ryu, C. Kim, C. Park, B.-S. Choi, J. Am. Chem. Soc. 2004 (2004) 9180.
36. C.-E. Lin, C.-J. Yu, C.-L. Chen, L.-D. Chou, C. Chou, J. Phys. Chem. A 114 (2010) 1665.
37. A. Gilbert, V. Silvestre, R.J. Robins, G.S. Remaud, Anal. Chem. 81 (2009) 8978.
38. G. Bodenhausen, D.J. Ruben, Chem. Phys. Lett. 69 (1980) 185.
39. I.A. Lewis, S.C. Schommer, B. Hodis, K.A. Robb, M. Tonelli, W. Westler, M. Sussman, J.L. Markley, Anal. Chem. 79 (2007) 9385.
40. R.R. Ernst, G. Bodenhausen, A. Wokaun, Principles of nuclear magnetic resonance in one and two dimensions, Oxford Science Publications ed., Oxford (1987).

Cite this article as:

Patrick Giraudeau *et al.*: **Ultrafast 2D NMR applied to the kinetic study of D-glucose mutarotation in aqueous solution.** *J. Spectrosc. Dyn.* 2011, **1**: 2